# Mobilized Electrospray Device for On-Tissue Chemical Derivatization in MALDI-MS Imaging

Andrew E. Paulson<sup>a,b</sup>, Evan A. Larson<sup>a,c</sup>, Young Jin Lee<sup>a</sup>\*

**ABSTRACT:** Applying solutions of matrix or derivatization agent via microdroplets is a common sample preparation technique for matrix-assisted laser desorption/ionization-mass spectrometry imaging (MALDI-MSI) experiments. Mobilized nebulizer sprayers are commonly used to create a homogeneous matrix or reagent layer across large surfaces. Electrospray devices have also been used to produce microdroplets for the same purpose but are rarely used for large tissues due to their immobility. Herein, we present a movable electrospray device that can be used for large tissue sample preparation by a simple modification to an automatic commercial nebulizer device. As demonstrated for on-tissue chemical derivatization (OTCD) with Girard's reagent T using a mimetic tissue model, the sprayer has the additional benefit of being able to investigate reaction acceleration in OTCD when comparing electrostatically charged spray to electrostatically neutral spray. Finally, MALDI-MSI of fatty aldehydes is successfully demonstrated in rat brain tissues using this device for both OTCD and matrix application.

**KEYWORDS:** On-tissue Chemical Derivatization, Electrospray, Reaction Acceleration, Mass Spectrometry Imaging

#### INTRODUCTION

Chemical derivatization is a common technique in analytical workflows with an aim to improve analyte response by introducing molecular functionalities that take the susceptibilities of a given analysis into account. Given the small sampling size and ion suppression caused by other molecular species in the sampled area during mass spectrometry imaging (MSI) experiments, amongst other issues, the MSI community often utilizes on-tissue chemical derivatization (OTCD) strategies to increase the ionization efficiency of poorly ionizing or dilute analytes of interest. <sup>1,2</sup> Derivatizing analytes with a reagent containing a permanent charge or highly ionizable group improves the detection and identification of target compounds during MSI analysis.

Derivatization for matrix-assisted laser desorption ionization-MSI (MALDI-MSI) experiments typically involves pneumatically spraying a solution of the derivatization reagent onto a dry sample. Specifically, a microdroplet solution containing the solvated derivatization reagent comes into contact with the surface, the reaction occurs between the reagent and analyte, and then the droplet dries, leaving the derivatized analyte. In this case, the reaction time is inherently limited by the drying of the droplets containing the reagent. As such, it is necessary to have a fast surface reaction to maximize the reaction efficiency.

Minimizing the size of the droplets that reach the sample surface is important for MALDI-MSI in order to limit analyte diffusion. Thus, the size of pneumatically sprayed droplets is intentionally very small by the time they arrive at the tissue surface due in part to solvent evaporation during droplet flight

time. Another common method to make microdroplets is electrospraying. As in electrospray ionization (ESI), a high voltage is applied to the spray solution, and the electric field at the tip of the needle produces a Taylor cone from the liquid, resulting in a spray of charged microdroplets. Unlike ESI-MS, the goal of electrospray in OTCD is to retain the solvation of solutes to allow for droplets to reach the sample surface and react. Though increasing OTCD reaction time and avoiding analyte diffusion are at odds, OTCD using either pneumatic sprays or electrosprays feature microdroplet and thin-film-like conditions, which have been shown to have improved reaction efficiency compared to bulk conditions.

According to Yan et al.,4 there are three main factors that influence reaction acceleration in microdroplets and thin films. The first is solvent evaporation leading to an increase in reagent concentration. Another factor is pH, as the pH within a microdroplet or thin film pH can become extreme compared to bulk. Similar to reagent concentration enrichment, this can simply be due to desolvation and increase in proton concentration, as shown in Girod et al., where pH decreased from 3.3 in bulk to 0.5 in secondary droplets in desorption electrospray ionization (DESI).<sup>5</sup> In electrospray-generated microdroplets, this can also be due to the electrolysis of water. This was demonstrated by Banerjee et al., where a reaction requiring acid was accelerated in positively charged microdroplets without the addition of an external acid.<sup>6</sup> The final acceleration effect is when the reaction is favored at the air/surface interface due to a lower activation energy or lower reaction entropy.<sup>5</sup> Many studies on reaction acceleration have focused on reactions in microdroplets in ESI or

<sup>&</sup>lt;sup>a</sup>Department of Chemistry, Iowa State University, Ames, IA 50011, USA

<sup>&</sup>lt;sup>b</sup>Present Address: Department of Chemistry, Saginaw Valley State University, University Center, MI 48710, USA

<sup>&</sup>lt;sup>e</sup>Present Address: Department of Horticulture Science, University of Minnesota, St Paul, MN 55108, USA

surface reactions in DESI. These include studies by Girod et al.<sup>5</sup> and Badu-Tawaih et al.,<sup>7</sup> who used reactive DESI or ambient soft charged-droplet landing to study the reaction of sprayed Girard's T (GT) with solid ketosteroids, among other reactions. They found that the acid-catalyzed GT reaction was accelerated in positively charged droplets, which can be attributed to either a pH decrease or the high concentration of reactants.

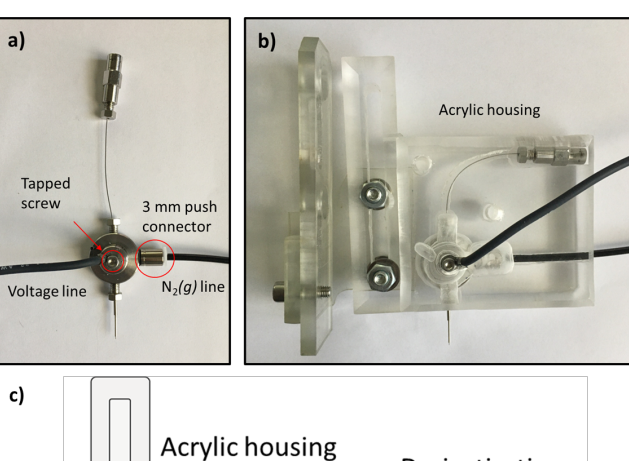
Only a few works have used electrospray as a sample preparation technique for MALDI-MS. Some studies used it for matrix deposition, 8,9 and others for OTCD. Guo et al. applied GT and 4-hydroxy-3-methoxycinnamaldehyde (CA) to tissue surfaces for OTCD via electrospray in their novel laser-assisted tissue transfer system. 10 Wu et al. compared electrospray vs. airbrush deposition of 2-picolylamine OTCD reagent onto rat cerebrum tissue and found that electrospray application led to a three-fold improvement in signal and less analyte delocalization.<sup>3</sup> Finally, Dueñas et al. found a four-fold improvement in unique spectral features with electrospray deposition compared to TM sprayer deposition for GT derivatization. 11 As both the neutral and charged spray depositions result in heterogeneous reaction systems that feature similarities of producing thin films as the individual droplets dry on surface, 7,12,13 improvement in reaction efficiency compared to bulk is anticipated for both. However, no work has focused on directly investigating and discussing the improved reaction efficiency between a charged spray and a neutral pneumatic spray for MALDI derivatization.

In this work, we develop an electrospray device that utilizes some of the TM sprayer hardware and software for movement. This system allows us to homogenously electrospray OTCD reagents onto a large tissue surface. Using a maize mimetic tissue model spiked with progesterone, the conversion efficiencies are directly compared between electrospray and neutral spray for the GT OTCD of progesterone. Lastly, similar performance is demonstrated in MALDI-MSI of rat brain tissues when electrospray application is compared to neutral spray application for GT OTCD.

#### **EXPERIMENTAL SECTION**

Chemicals. Girard's Reagent T (GT) (>99.0%) trifluoroacetic acid (TFA)(>99.5%), progesterone (>99%), and gelatin from porcine skin (gel strength 300, Type A) were purchased from Sigma Aldrich (St. Louis, MO, USA). 2,5-dihydroxybenzoic acid (99%) and LC-MS grade water were purchased from Alfa Aesar (Ward Hill, MA, USA). HPLC grade methanol was purchased from Fisher Chemical (Pittsburg, PA, USA). Glycerol (99.7%) was purchased from VWR (Radnor, PA, USA).

Electrospray Device. An ESI sprayer, PN: 017614, from a retired mass spectrometer (OSTAR, SCIEX, Framingham, MA, USA) was modified and mounted to the TM-Sprayer (HTX Technologies, Chapel Hill, NC, USA) translation arm (Figure 1). Three modifications were made in total. The three-way metal junction that introduces the sheath gas around the metal capillary was tapped to allow for a screw connection for voltage application. The PTFE sheath gas connection was replaced with a push fitting (PISCO, Elk Grove Village, IL, USA) to accommodate the 3 mm nitrogen line on the TM sprayer. An acrylic housing was made to insulate the electrospray device and to allow attachment to the TM sprayer x-y positioning arm. An acrylic box was also made to insulate a metal sample platform from the base of the TM sprayer (Figure 2). A high voltage was applied to the electrospray device while the sample base plate was grounded.



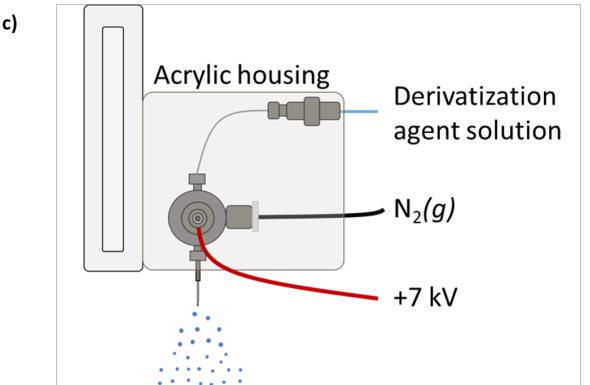
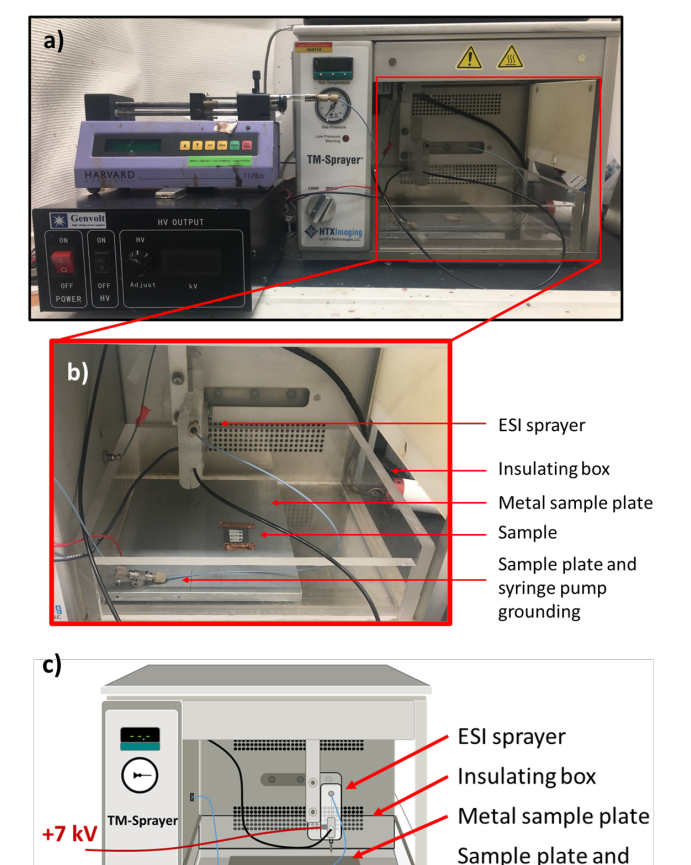


Figure 1. (a) ESI sprayer head, (b) acrylic housing, and (c) schematic of assembled electrospray device.



**Figure 2.** (a) Mounted ESI sprayer, (b) modified sample stage, and (c) a schematic of the assembled mobilized electrospray device.

syringe pump

grounding

Droplet Size Comparison. A typical spray solvent, 70:30 mixture of MeOH and 0.1% TFA (v/v), was mixed with glycerol at 90:10 (v/v). This mixture was used to measure droplet size based on previous work by Hollerbach et al. 14 Glass microscope slides were pre-sputtered for 10 seconds with a platinum target using a sputter coater (Cressington 108 Auto Sputter Coater, Ted Pella Inc., Redding, CA, US) to provide conductivity for the slides. A one-line pass over the Pt coated glass slides was programed using the TM Sprayer software for both the electrospray device and TM sprayer head. Both sprayers were operated at a 0.03 mL/min flow rate and 1200 mm/min velocity. The parameters specific to the electrospray device were a nitrogen pressure of 25 psi, a spray voltage of +7kV, and operated at room temperature (~21°C). The parameters specific to the TM sprayer were a nitrogen pressure of 10 psi and an operation temperature of 30°C.

Mimetic tissue Microarray. Maize B109 plants were grown following previously published methods. Briefly, eight maize B109 seeds were wrapped in a damp paper towel and placed into a graduated cylinder with ~50 mL of water in an incubator kept at 25 °C. <sup>15</sup> After two weeks of growth, the roots and shoots of the plants were diced and combined. About 500 mg of plant tissues with a 5 mm stainless steel bead were added into each of twelve tubes, and homogenized at 50 Hz using the TissueLyser LT (Qiagen, Germantown, MD, USA) for 20 minutes. During

homogenization, each tube was centrifuged at 14,000 rpm for 10 seconds every five minutes to remove the tissue from the top of the tube. After initial homogenization, all twelve tubes were combined into a single 50 mL centrifuge tube and the homogenized tissues were aliquoted into  $\sim\!200$ - 300 mg portions. Two solutions of progesterone in methanol were made at 30 mg/mL and 15 mg/mL. One of these solutions was then added to an aliquot of homogenized tissue at 1  $\mu L/10$  mg for a final concentration of 30 ng progesterone per mg maize homogenate or 15 ng/mg. The spiked maize homogenate aliquots were then homogenized for another 20 minutes with centrifugation every five minutes using settings specified above.

A 20% porcine gelatin solution (w/v) was made in water by heating at ~70 °C until clear. The hot gelatin solution was poured into a 36 core (3mm diameter) silicone T-Sue<sup>TM</sup> microarray mold (Simport Scientific, Beloeil, QC, Canada), and allowed to cool for 20 minutes in a 4°C refrigerator. After cooling, the gelatin microarray was removed from the mold and cut into sections with 3x3 wells. Three wells were filled with each concentration for the spiked maize homogenate to produce three replicates. After filling each well, the tissue microarray was flash frozen with liquid nitrogen and stored at -80°C. Frozen tissue microarrays were transferred to a cryostat (CM 1850, Leica Microsystems, Buffalo Grove, IL, USA) at -20°C and sectioned to 20 μm. Tissue microarray sections were thaw mounted onto Pt coated glass slides and vacuum dried on a prechilled steel block (-80°C) for 1.25 hours.

Sample Preparation for Conversion Efficiency Experiment. For pH experiments, a 10 µM GT solution was made in 70:30 mixture of MeOH and aqueous solutions of TFA at various concentrations (0%, 0.001%, 0.01%, and 0.1%, v/v). For GT concentration experiments, 0.10  $\mu M$ , 1.0  $\mu M$ , 10  $\mu M$ , 0.10 m M, and 1.0 mM GT in 70:30 MeOH:0.1%TFA were prepared. For the experiments comparing typical derivatization reagent concentrations. GT solution was made at 10 mg/mL in 70:30 MeOH:0.1% TFA. GT solutions were sprayed using the same spray method (6 passes, 0.03 mL/min flow rate, 1200 mm/min velocity, 3 mm track spacing, using a crisscross pattern) using either the TM sprayer head or the electrospray device. The TM-Sprayer head N<sub>2</sub>(g) pressure was kept at 10 psi while the ESI pressure was kept at 25 psi to maintain spray integrity. The TM-Sprayer nozzle was at 30°C while the electrospray device was at room temperature (~21°C). The electrospray spray voltage was set to +7 kV using a high-voltage power supply (Genvolt, Boston, MA, USA). After applying derivatization reagent, 2,5dihydroxybenzoic acid (DHB, 40 mg/mL) in 70:30 MeOH:0.1% TFA was sprayed using the TM-Sprayer (75°C nozzle temperature, 8 passes, 0.1 mL/min flow rate, 1200 mm/min velocity, 3 mm track spacing, using a crisscross pattern). For the experiments comparing typical derivatization reagent concentrations, some samples had matrix applied with the electrospray device at +7 kV and 25 psi for N<sub>2</sub>(g) using the same DHB solutions and TM-Sprayer method used for the TM-Sprayer matrix application. Control samples without OTCD were prepared by applying only matrix via TM-Sprayer or electrospray device.

Rat Brain Fatty Aldehyde Derivatization Experiments. Thawmounted 15 µm thick rat brain sections on ITO slides were placed on a prechilled steel block (- 80°C) and dried for 1.25 hours under vacuum. A reagent solution of 10 mg/mL GT in 70:30 MeOH:0.1% TFA was sprayed onto the samples using the electrospray device or TM-Sprayer using the parameters

specified above. A matrix solution of 40 mg/mL DHB in 70:30 MeOH: $\rm H_2O$  was sprayed onto the samples using the electrospray device or TM-Sprayer using the parameters specified above for matrix application. Control samples without OTCD were prepared by applying only matrix via TM-Sprayer or electrospray device.

Mass Spectrometry and Data Analysis. Tissue microarrays and rat brain tissue samples were analyzed on a MALDI source (Spectroglyph, Kenniwick, WA, USA) coupled to a Q Exactive HF Orbitrap mass spectrometer (Thermo, San Jose, CA, USA). All mimetic tissue arrays were analyzed at 100 µm raster step at a scan range of m/z 100 – 750 with the resolution of 120,000 at m/z 200. All brain tissues were analyzed at 50  $\mu$ m raster step at a scan range of m/z 100 – 1200, and using a resolution of 120,000 at m/z 200. After data collection, .imzML files were generated using ImageInsight (Spectroglyph). The datasets from mimetic tissue arrays were loaded into MSiReader v1.02 (NC State, Raleigh, NC, USA) and selected masses were extracted from the same size region of interest. The datasets for the GT-derivatized rat brain were uploaded onto METASPACE (https://metaspace2020.eu/project/GT OTCDwESIorTM) and the TM sprayer derivatized dataset was searched against the LipidMaps database at 20% FDR, ±3 ppm mass tolerance, and "+C<sub>5</sub>H<sub>12</sub>N<sub>3</sub>" in the chemical modification tool. Images of selected annotated derivatized m/z were generated with a  $\pm 4$  ppm in MSiReader for all rat brain samples.

#### RESULTS AND DISCUSSION

Electrospray Device Construction. Typical OTCD sample preparation is done using a TM-Sprayer or similar pneumatic device with sprayer head movement, providing a homogenous coating of derivatization agents across the tissue surface. Static electrospray systems are difficult to compare to the neutral TM-Sprayer as the amount of reagent deposited can vary depending on the distance from the center of the spray. Previously reported electrospray devices are stationary, and the sample stage is moved instead.<sup>8–10</sup> In this work, we designed an electrospray device that could be directly mounted to the TM-Sprayer arm in order to utilize the same translation motor and software. The electrospray device head was built by encasing the ESI needle and sheath gas junction from a SCIEX ESI source into an acrylic housing to provide a mountable surface and to insulate the sprayer, minimizing shock hazards (Figure 1 and 2). The same sheath gas and syringe pump connections from the TM-Sprayer are used with the electrospray device. A high voltage (+7 kV) is applied to the sprayer head by a wire screwed into the metal sheath gas junction. The electrospray device and acrylic housing are then connected to the TM-Sprayer arm to allow for translation across the sample. The metal capillary tip is positioned 3 cm above the sample surface. In addition to being simple to construct, this design also provides a more robust comparison to the TM-Sprayer, ensuring that the same amount of derivatization reagent is applied between the two techniques as the same spray program can be used for each sprayer head.

Though the amount of reagent and flow rate of solution are the same, several parameter changes for optimal electrospray device operation make an exact comparison between the sprayers limited. One limitation of the spray setup is that this electrospray needle and sheath gas were designed as an ionization source, and as a result, a higher sheath gas pressure is necessary for a coherent nebulized spray. The TM-Sprayer pressure for our typical derivatization methods is 10 psi, while the pressure

for the electrospray device for derivatization is 25 psi. As the electrospray sheath gas push connection was selected to be compatible with the TM-Sprayer gas line, the pressure can be precisely controlled. The nitrogen pressure difference is anticipated due to differences in the sprayer construction. For instance, the electrospray emitter tip has an inner diameter of 200 μm and outer diameter of 400 μm, and the inner diameter for the sheath gas is 500 µm. In contrast, the TM-Sprayer capillary has an inner diameter of 100 μm and outer diameter of 250 μm, and the inner diameter for the sheath gas is 600 µm. Another limitation is that we currently do not have a way to heat the electrospray device. Therefore, the temperature of the electrospray sprayer head is at room temperature (~21°C) while the TM Sprayer head is held at 30 °C through the built-in hardware and software controls. Although the sheath gas pressure is different between the two methods and temperatures vary slightly, the liquid flow rate and spray method (sprayer head movement, track spacing, and pattern) are the same so the amount of derivatization reagent deposited is equivalent. The other clear difference is the application of voltage to the electrospray device, which is the main parameter that we are investigating. This was optimized to +7 kV, the minimum voltage required for a stable Taylor cone at the spray tip without sheath gas. Higher voltages may also be effective, but a minimum voltage was used as a safety precaution.

Comparison of Droplet Size. A 90:10 (v/v) mixture of our typical spray solvent (70:30 MeOH:0.1% TFA) and glycerol was used to measure droplet size based on previous work by Hollerbach *et al.*. <sup>14</sup> The confocal images of the glycerol droplets for the TM-Sprayer and electrospray device are shown in **Figure 3**. The droplet size is much smaller for the electrospray, which is mostly due to the Coulombic fission of the droplets. Importantly, the smaller droplets produced by the electrospray device would allow for smaller resulting crystal size during matrix application and also minimize on-tissue analyte diffusion during the application of the derivatization agent, improving maximum MSI spatial resolution.

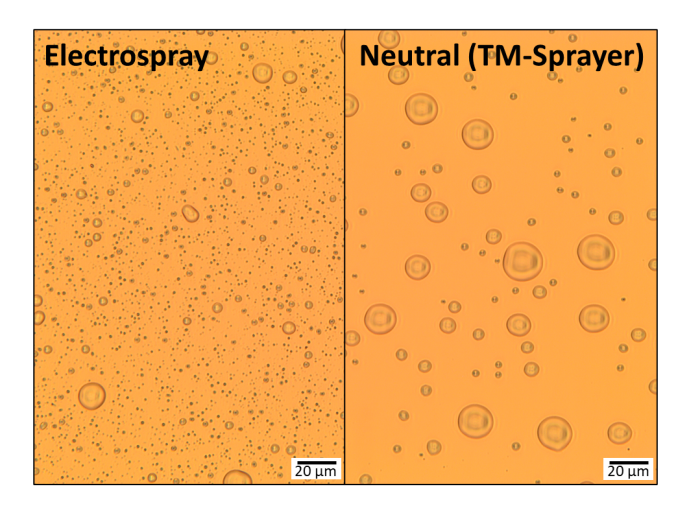


**Figure 3.** Microdroplet size generated from electrospray and neutral spray (TM-Sprayer).

Mimetic Maize Tissue Microarray. The first challenge in comparing sample preparation techniques for MSI is to prepare surfaces with reproducible standard compound distributions that allow for a fair comparison. Spotted standards tend to dry inconsistently, leading to matrix effects and inconsistent sample

thickness. Thus, spotted standards can have artifacts in the data that can lead to misinterpretation and increased analytical variation. For this reason, we adapted the mimetic tissue model previously developed for drug quantification in mammalian tissues. <sup>16,17</sup> We use a mimetic tissue microarray made of homogenized maize roots and shoots in this study (**Figure 4**). Two separate aliquots of homogenate were spiked with progesterone, a standard that reacts well with GT. Progesterone tissue densities of 15ng/mg and 30ng/mg were investigated in the mimetic tissue microarray with three replicates each. These mimetic models serve as a useful sample for quantifying the conversion efficiency difference between TM-Sprayer and electrospray device. In addition, this is the first mimetic tissue model developed using plants and the methodology developed here will be useful for quantification in other plant imaging applications.



### 5<sub>m</sub>m

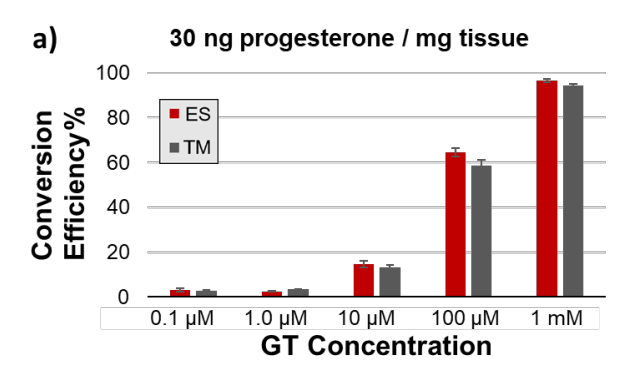
**Figure 4.** Example of 20 μm thick cryosectioned and thaw-mounted maize mimetic tissue array for three replicates of 30ng progesterone/mg of tissue homogenate.

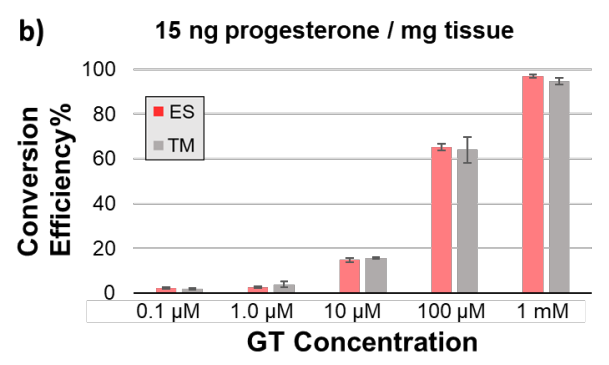
Reaction Efficiency Investigation. Using the electrospray device and mimetic tissue model described above, we compared the TM-Sprayer and electrospray device for GT reaction efficiency. GT is a positively charged derivatization reagent containing a hydrazine group. The hydrazine group undergoes an acid-catalyzed dehydration reaction with ketones and aldehydes (Scheme 1).

Scheme 1. Girard's T Derivatization of Progesterone

To assess the difference in reaction efficiencies, GT is sprayed at a low concentration (10  $\mu M)$  on purpose to leave some progesterone underivatized (**Figure 5**). This concentration is six thousand times less than typically used in OTCD (10 mg/mL) in order to allow for the calculation of the conversion efficiency (CE) from unreacted analytes. Here, we define CE as the product ion signal divided by the ion signals of both reacted and unreacted analyte:

$$CE = \frac{[M+GT-H_2O]^+}{[M+GT-H_2O]^+ + [M+H]^+ + [M+Na]^+} \times 100$$
 (eqn. 1)

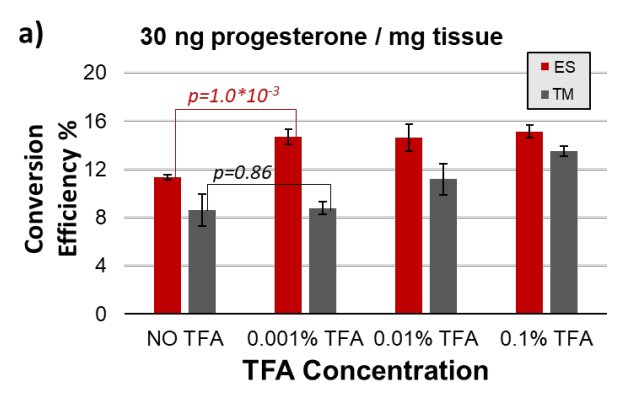




**Figure 5**. Conversion efficiency of derivatization using various GT concentrations in 70:30 MeOH:0.1%TFA with a target analyte, progesterone, tissue density of **(a)** 30 ng/mg or **(b)** 15 ng/mg.

The product has a permanent charge in GT, [M+GT-H<sub>2</sub>O]<sup>+</sup> (*m*/*z* 428.327), and the unreacted analyte is detected as the protonated or sodiated adduct, [M+H]<sup>+</sup> (*m*/*z* 315.232) or [M+Na]<sup>+</sup> (*m*/*z* 337.214), respectively. It should be noted that CE is only a rough estimation of the reaction efficiency because the ionization efficiency difference is ignored for simplicity. As progesterone has a lower ionization efficiency without derivatization, CE overestimates the true reaction efficiency. However, CE should be sufficient for the purpose of comparing the relative efficiencies of the same OTCD reaction between the TM-Sprayer and the electrospray device.

**Figure 6** demonstrates the higher CE with the electrospray device when compared to the TM-Sprayer when there are different amounts of TFA in the sprayed solvent. Most importantly, there is a significant improvement in CE with ESI between no TFA and 0.001% TFA for both the mimetic tissues, but it is not significant with the TM-Sprayer. Furthermore, there is no improvement at higher TFA concentrations with electrospray, suggesting that the reaction may have reached the maximum CE with the given GT concentration. In contrast, CE continuously increased with TM-Sprayer as higher TFA concentrations were used. Yet, in all cases, the CE of GT OTCD while using the TM-sprayer is still lower than that of the CE while using electrospray. Consistent with these findings, both methods have comparable CEs when using 0.1% TFA regardless of the GT concentrations (**Figure 5**).



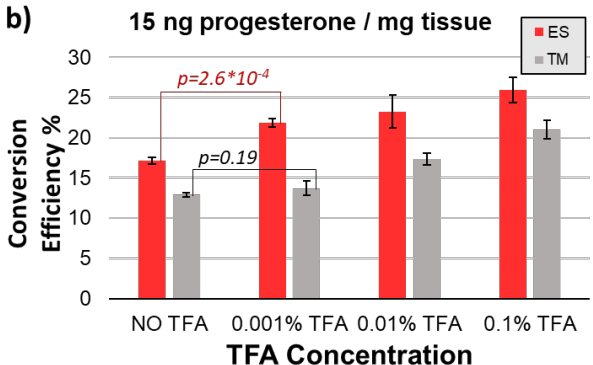


**Figure 6.** Conversion efficiency of progesterone in mimetic tissue microarray with a progesterone density of (a) 30 ng/mg or (b) 15 ng/mg. GT concentration was 10  $\mu$ M in 70:30 MeOH:various TFA (v/v).

Reaction acceleration is expected for both sprayers due to the generation of microdroplets and thin-film-like conditions as the droplets dry. The observation that adding small amounts of TFA gave larger improvements for electrospray conversion efficiency when compared to neutral spray is likely due to the two factors leading to lower pH in electrospray generated droplets. The smaller size of the charged microdroplets results in faster evaporation due to the larger surface-to-volume ratio, leading to the higher proton concentrations in the droplets hitting the sample surface. Additionally, the acid catalyzed GT reaction has a higher CE for electrospray even without TFA probably due to the electrolytic oxidation of water.<sup>6</sup> All considered, the evidence of smaller droplet size in Figure 3 and the significance of TFA concentration in Figure 6 suggest the pH characteristics of the charged droplets are the major contributor to the higher CE with electrospray for GT OTCD.

Another way to compare the two reaction efficiencies is through relative conversion efficiency (RCE):

$$RCE = \frac{CE \text{ of } Electrospray}{CE \text{ of } Neutral Spray}$$
 (eqn. 2)

As both the sprays induce the reaction acceleration compared to the bulk phase reaction, the RCE more clearly indicates additional improvements specific to the electrospray. As shown in **Figure 7**, RCE is always greater than one but is largest at 0.001% TFA, then becomes closer to one as TFA concentration increases, again suggesting pH is the major factor for the high reaction efficiency with electrospray in the case of GT OTCD.

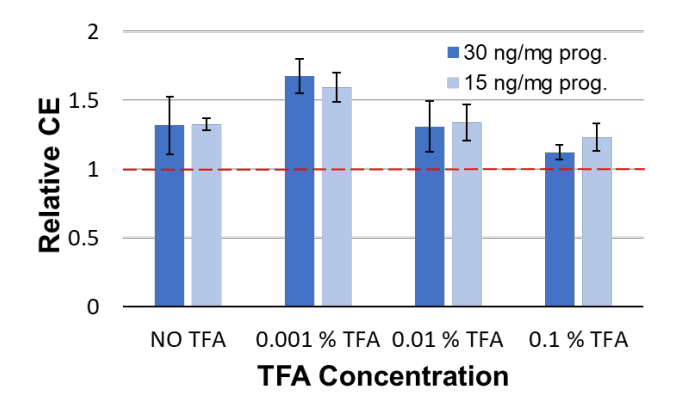


**Figure 7.** Relative conversion efficiency of electrospray vs. neutral spray from the data in Figure 6.

Though there are some differences, the reaction acceleration observed in reactive DESI with GT is also driven, partially, by pH effects of the microdroplets. 5 GT OTCD of progesterone with electrospray is also similar to the soft-landing of charged microdroplets containing GT onto solid ketosteroids demonstrated by Badu-Tawiah et al., where reaction rate improvement was attributed to droplet charge and resulting pH effects due to the positive voltage used to generate the droplets. In the softlanded droplet reaction system, Badu-Tawiah et al. mentioned that microsolvation of the reagents occur as the droplets evaporate in the air and during the droplet residence time on the solid surface, where longer microsolvation on the sample surface can lead to an increase in product yield. Extending these previous findings and interpretations to our reaction system suggests pH differences in charged microdroplets account for the differences, while the thin film and microdroplet acceleration characteristics account for the generally observed GT reaction when using the charged and neutral droplets.

Comparison of TM-Sprayer and Electrospray Device for Typical Derivatization Conditions. When using high enough concentrations that are typical for most GT OTCD, 10 mg/ml GT with 0.1%TFA, 18 the CEs are almost 100% and there is no statistical difference between using the electrospray device and the neutral spray (**Figure 8**). Given the known effectiveness of GT derivatization protocols for MSI, this is expected.

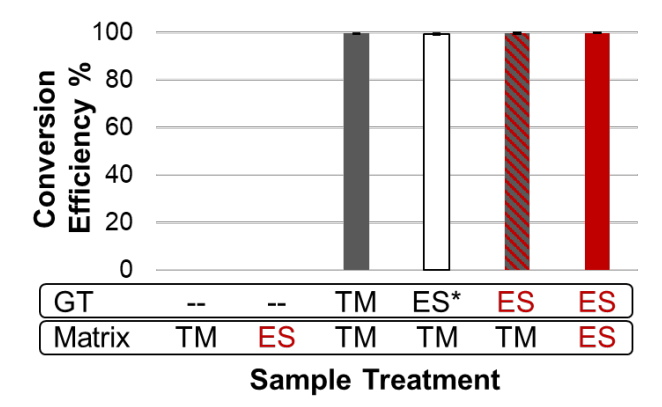


**Figure 8.** Conversion efficiency of progesterone in the mimetic tissue microarray (30 ng/mg) for the GT OTCD with typical derivatization reagent concentrations (10mg/ml). OTCD and matrix

application were made by the electrospray device (ES) or TM-Sprayer (TM) as indicated; GT application (top) and matrix application (bottom). The \* indicates that the electrospray device was used without applying voltage.

No difference in CEs in **Figure 8** is attributed to the bulk characteristics of the droplets. When TFA and GT concentrations are large enough, there is an abundance of protons and GT in both conditions, so the benefit of electrospray is lost. Regardless, the electrospray device has no detrimental effects on the conversion efficiency using typical reagent concentrations. Some benefits are expected for the electrospray device by using lower concentrations of derivatization agents to minimize ion suppression. Another benefit is its smaller droplet size that minimizes the diffusion of analytes on the tissue surface. Though the GT reaction goes to complete conversion, other derivatization reactions have poor reaction yields and may benefit from applications with electrospray. Future work will investigate these derivatization systems.

Application to OTCD for Imaging Experiment. To demonstrate the application of this electrospray system to large tissue samples, GT derivatization was performed on thaw mounted rat brain sections with electrospray device or TM-Sprayer and DHB matrix was applied also with electrospray device or TM-Sprayer (Figure 9). When using the recently developed METASPACE derivatization annotation tool, <sup>18</sup> fatty aldehydes (FAL) are readily observed as derivatized features in the tissue. Recently, FAL in this tissue type were suggested to fluctuate between healthy individuals and those with diabetic encephalopathy, where localizations were visualized using air-flow-assisted DESI-MS imaging using GT derivatization.<sup>19</sup> As shown in Figure 9a, there is no FAL detected without OTCD but FAL 16:0, 18:1, and 18:0 were readily detected with GT OTCD. The localization of the fatty aldehydes is similar regardless of how GT is applied but overall signal is better when electrospray device is used. Minimal signal improvement of derivatized signal for the electrospray GT application samples is attributed to sample variation, given the results from the mimetic tissue microarray experiments.

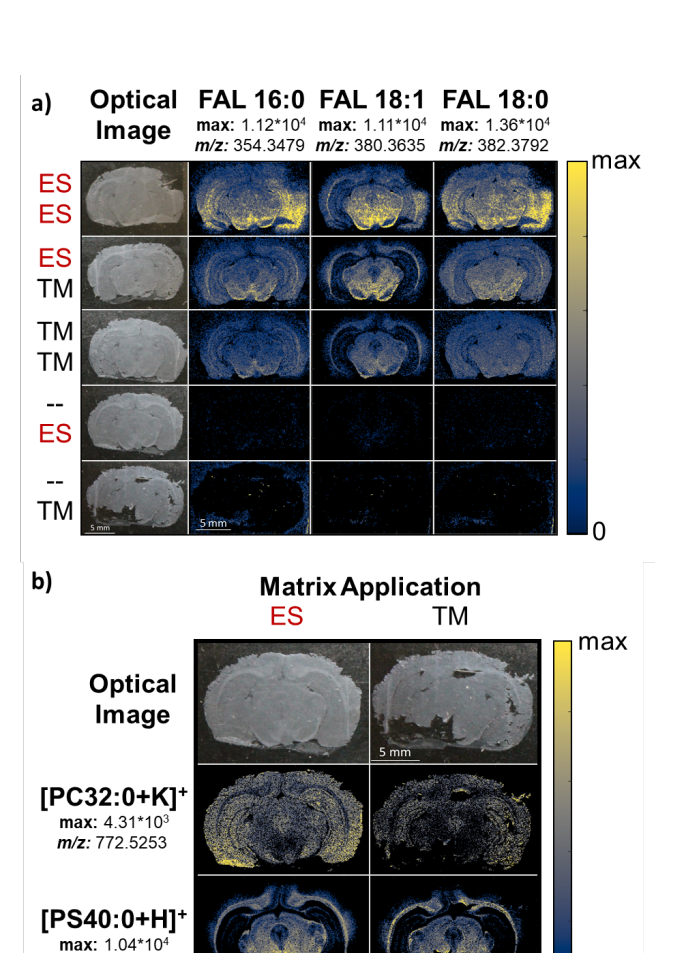


**Figure 9. (a)** OTCD MALDI-MS images of fatty aldehydes in rat brain tissues. Electrospray device (ES) or TM-Sprayer (TM) was used for GT application (top) and matrix application (bottom) as indicated on the left. The bottom two rows only have matrix applied. **(b)** MALDI-MS images of other lipids without derivatization that demonstrate similar spatial localizations.

It appears that there may be analyte delocalization, specifically FAL 18:1, when using the electrospray device for derivatization and the matrix application (Figure 9a). However, when using the electrospray device for matrix application alone, the analyte localization of other lipids do not have significant differences (Figure 9b). Additionally, there is minimal diffusion of the analytes into regions off the tissue for any of the derivatized FALs. Further experiments would be necessary, but the observed localization difference was tentatively attributed to the slightly higher signals in this replicate. Collectively, the results suggest that delocalization issues are minimal at worst, and minor differences are likely due to signal variations rather than the characteristics of the spray. Thorough evaluation of spatial resolution is challenging with the current instrumentation as the spatial resolution is limited to the ~15 µm laser spot size but could be performed in the future with laser spot size improvement.

#### **CONCLUSIONS**

m/z: 848.6375

In this work, we developed an electrospray device setup mountable to an existing automatic pneumatic sprayer that can be used for matrix application or OTCD. Using mimetic tissue microarrays as homogenous tissue surrogates, the reaction acceleration

in OTCD was investigated for the electrospray device compared to neutral spray. For GT OTCD, the main improvement of conversion efficiency is attributed to the pH effect in electrospray-generated microdroplets. The minimum variation in the obtained efficiencies suggests the mimetic tissue model is more reliable than standard spotting, which suffers from coffee ring effects. We also demonstrate the use of the sprayer at typical reagent concentrations both on our mimetic model and on large tissue areas. Future studies will utilize this system to investigate other derivatization reactions, focusing largely on acid (positive sprayer potential) and base (negative sprayer potential) catalyzed reactions.

#### **ACKNOWLEDGEMENT**

This material is based upon work supported by the National Science Foundation under Grant No. 1905335.

#### **AUTHOR INFORMATION**

#### Corresponding Author

\* To whom correspondence should be addressed: Tel: 515-294-1235, Email: <a href="mailto:yilee@iastate.edu">yilee@iastate.edu</a>

#### **Author Contributions**

YL conceived the idea. AP and EL designed and performed the experiments and data analysis. The manuscript was written through contributions of all authors. All authors have given approval to the final version of the manuscript.

#### **REFERENCES**

- (1) Harkin, C.; Smith, K. W.; Cruickshank, F. L.; Logan Mackay, C.; Flinders, B.; Heeren, R. M. A.; Moore, T.; Brockbank, S.; Cobice, D. F. On-tissue Chemical Derivatization in Mass Spectrometry Imaging. *Mass Spectrometry Reviews* 2022, 41 (5), 662–694. https://doi.org/10.1002/mas.21680.
- (2) O'Neill, K. C.; Dueñas, M. E.; Larson, E.; Forsman, T. T.; Lee, Y.-J. Enhancing Metabolite Coverage for Matrix-Assisted Laser Desorption/Ionization Mass Spectrometry Imaging Through Multiple On-Tissue Chemical Derivatizations. In Mass Spectrometry Imaging of Small Molecules; Lee, Y.-J., Ed.; Methods in Molecular Biology; Springer US: New York, NY, 2022; Vol. 2437, pp 197–213. https://doi.org/10.1007/978-1-0716-2030-4\_14.
- Wu, Q.; Comi, T. J.; Li, B.; Rubakhin, S. S.; Sweedler, J. V. On-Tissue Derivatization via Electrospray Deposition for Matrix-Assisted Laser Desorption/Ionization Mass Spectrometry Imaging of Endogenous Fatty Acids in Rat Brain Tissues. Anal. Chem. 2016, 88 (11), 5988–5995. https://doi.org/10.1021/acs.analchem.6b01021.
- (4) Yan, X.; Bain, R. M.; Cooks, R. G. Organic Reactions in Microdroplets: Reaction Acceleration Revealed by Mass Spectrometry. *Angew. Chem. Int. Ed.* 2016, 55 (42), 12960–12972. https://doi.org/10.1002/anie.201602270.
- (5) Girod, M.; Moyano, E.; Campbell, D. I.; Cooks, R. G. Accelerated Bimolecular Reactions in Microdroplets Studied by Desorption Electrospray Ionization Mass Spectrometry. Chem. Sci. 2011, 2 (3), 501–510. https://doi.org/10.1039/C0SC00416B.
- Banerjee, S.; Zare, R. N. Syntheses of Isoquinoline and Substituted Quinolines in Charged Microdroplets. *Angew. Chem.* 2015, 127 (49), 15008–15012. https://doi.org/10.1002/ange.201507805.

- (7) Badu-Tawiah, A. K.; Campbell, D. I.; Cooks, R. G. Reactions of Microsolvated Organic Compounds at Ambient Surfaces: Droplet Velocity, Charge State, and Solvent Effects. J. Am. Soc. Mass Spectrom. 2012, 23 (6), 1077–1084. https://doi.org/10.1007/s13361-012-0365-3.
- (8) Guo, S.; Wang, Y.; Zhou, D.; Li, Z. Electric Field-Assisted Matrix Coating Method Enhances the Detection of Small Molecule Metabolites for Mass Spectrometry Imaging. *Anal. Chem.* 2015, 87 (12), 5860–5865. https://doi.org/10.1021/ac504761t.
- (9) Li, S.; Zhang, Y.; Liu, J.; Han, J.; Guan, M.; Yang, H.; Lin, Y.; Xiong, S.; Zhao, Z. Electrospray Deposition Device Used to Precisely Control the Matrix Crystal to Improve the Performance of MALDI MSI. *Sci Rep* 2016, 6 (1), 37903. https://doi.org/10.1038/srep37903.
- (10) Guo, S.; Tang, W.; Hu, Y.; Chen, Y.; Gordon, A.; Li, B.; Li, P. Enhancement of On-Tissue Chemical Derivatization by Laser-Assisted Tissue Transfer for MALDI MS Imaging. *Anal. Chem.* **2020**, *92* (1), 1431–1438. https://doi.org/10.1021/acs.analchem.9b04618.
- (11) Dueñas, M. E.; Larson, E. A.; Lee, Y. J. Toward Mass Spectrometry Imaging in the Metabolomics Scale: Increasing Metabolic Coverage Through Multiple On-Tissue Chemical Modifications. *Front. Plant Sci.* **2019**, *10*, 860. https://doi.org/10.3389/fpls.2019.00860.
- (12) Wei, Z.; Wleklinski, M.; Ferreira, C.; Cooks, R. G. Reaction Acceleration in Thin Films with Continuous Product Deposition for Organic Synthesis. *Angew. Chem. Int. Ed.* 2017, 56 (32), 9386–9390. https://doi.org/10.1002/anie.201704520.
- (13) Salvitti, C.; De Petris, G.; Troiani, A.; Managò, M.; Villani, C.; Ciogli, A.; Sorato, A.; Ricci, A.; Pepi, F. Accelerated D-Fructose Acid-Catalyzed Reactions in Thin Films Formed by Charged Microdroplets Deposition. *J. Am. Soc. Mass Spectrom.* 2022, 33 (3), 565–572. https://doi.org/10.1021/jasms.1c00363.
- (14) Hollerbach, A.; Logsdon, D.; Iyer, K.; Li, A.; Schaber, J. A.; Graham Cooks, R. Sizing Sub-Diffraction Limit Electrosprayed Droplets by Structured Illumination Microscopy. Analyst 2018, 143 (1), 232–240. https://doi.org/10.1039/C7AN01278K.
- (15) Feenstra, A. D.; Dueñas, M. E.; Lee, Y. J. Five Micron High Resolution MALDI Mass Spectrometry Imaging with Simple, Interchangeable, Multi-Resolution Optical System. *J. Am. Soc. Mass Spectrom.* 2017, 28 (3), 434–442. https://doi.org/10.1007/s13361-016-1577-8.
- (16) Groseclose, M. R.; Castellino, S. A Mimetic Tissue Model for the Quantification of Drug Distributions by MALDI Imaging Mass Spectrometry. *Anal. Chem.* 2013, 85 (21), 10099– 10106. https://doi.org/10.1021/ac400892z.
- (17) Barry, J. A.; Groseclose, M. R.; Castellino, S. Quantification and Assessment of Detection Capability in Imaging Mass Spectrometry Using a Revised Mimetic Tissue Model. *Bioa-nalysis* 2019, 11 (11), 1099–1116. https://doi.org/10.4155/bio-2019-0035.
- (18) Larson, E. A.; Forsman, T. T.; Stuart, L.; Alexandrov, T.; Lee, Y. J. Rapid and Automatic Annotation of Multiple On-Tissue Chemical Modifications in Mass Spectrometry Imaging with Metaspace. *Anal. Chem.* 2022, 94 (25), 8983–8991. https://doi.org/10.1021/acs.analchem.2c00979.
- (19) Meng, X.; Liu, Y.; Huo, M.; Yang, S.; Zhang, X.; Tian, L.; Li, W.; Wei, J.; Wang, Z.; Zhou, Z.; Chen, Y.; Wang, Z.; Abliz, Z. Mapping of Fatty Aldehydes in the Diabetic Rat Brain Using On-Tissue Chemical Derivatization and Air-Flow-Assisted Desorption Electrospray Ionization-Mass Spectrometry Imaging. J. Proteome Res. 2023, 22 (1), 36–46. https://doi.org/10.1021/acs.jproteome.2c00445.

## Table of Contents (TOC)

